J. Anat. (1995) 186, pp. 271–286, with 5 figures Printed in Great Britain

Morphometry of the primate bony labyrinth: a new method based on high-resolution computed tomography

FRED SPOOR[1] AND FRANS ZONNEVELD[2]

[1] *Department of Anatomy and Developmental Biology, University College London, UK, and* [2] *Department of Radiology, Utrecht University Hospital, Utrecht, The Netherlands*

(*Accepted 15 September 1994*)

ABSTRACT

A method is described for taking accurate measurements of the bony labyrinth of humans and other primates using high-resolution computed tomography (CT). The measurements comprise 8 dimensions, 14 orientations and 2 indices of the labyrinth, as well as 7 orientations of related structures of the petrous pyramid. Comparison of the measurements taken from CT scans with those taken from subsequently made casts and cryosections demonstrates that the method is sufficiently accurate to permit the morphometric analysis of labyrinthine size and shape. Since the CT method is nondestructive, fast and easy to perform, it is applicable to large samples and to rare or precious anthropological specimens.

Key words: Inner ear; labyrinth; computed tomography; morphometry.

INTRODUCTION

Morphometric studies of the primate bony labyrinth have been made for a variety of purposes. The oldest category concerns purely descriptive and comparative works, which first appeared following the discovery that the labyrinth can be studied by casting the air-filled spaces of the macerated temporal bone (Hyrtl, 1845; Siebenmann, 1890; Denker, 1899; Berg, 1903; Sato, 1903; Schönemann, 1906; Gray, 1907; Turkewitsch, 1930; Caix & Outrequin, 1976, 1979; Muren et al. 1986; Dimopoulos & Muren, 1990). A second category deals with those aspects of the labyrinth that have a direct biophysical relationship with the function of the vestibular organ, the dimensions and the planar orientations of the semicircular canals in particular (Igarishi, 1967; Igarishi et al. 1981; Blanks et al. 1975, 1985; Curthoys et al. 1977*a*, *b*; Ramprashad et al. 1984; Matano et al. 1985, 1986; Reisine et al. 1988). These studies are generally made to obtain morphological measurements that can be used in hydrodynamic models of endolymph and cupula movements, to calculate the sensitivity and time constants of the semicircular canal system. Finally, a third group of studies applies specific angular measurements to describe morphological features of the labyrinth that are said to be related to the ontogenetic and phylogenetic development of the cranial base. Examples are the orientations of the common crus (Werner, 1933), the interfenestral axis connecting the oval and round windows (Saban, 1952), and the ampullar plane through the 3 ampullae (Villemin & Beauvieux, 1934).

The bony labyrinth is one of the most difficult structures of the body to investigate, because its complicated 3-dimensional shape is hidden inside the dense otic capsule of the petrous bone. Consequently, morphometric analyses are based on casts, dissections and serial sections, and as these techniques are destructive they can only be used for the study of readily available material, such as laboratory animals (squirrel monkeys, macaques), or human petrous pyramids from the dissection room. Moreover, as the preparation of casts, dissections and serial sections requires both considerable skill and time, these techniques are not convenient for the study of large samples. In contrast, high-resolution computed tomography (CT) enables the structures of the inner ear to

Correspondence to Dr Fred Spoor, Department of Anatomy and Developmental Biology, University College London, Rockefeller Building, University Street, London WC1E 6JJ, UK.

be visualised in detail (Zonneveld, 1987; Sick & Veillon, 1988), is nondestructive, and the process of making CT scans of the temporal bone is relatively fast and easy to perform. Hence, if accurate measurements of the bony labyrinth can be taken from CT scans, it is the appropriate method for the morphometric analysis of this structure in large samples or in rare or precious anthropological specimens.

When comparing linear measurements of the human semicircular canals taken from CT scans with subsequently made casts, Muren & Ytterbergh (1986) noted CT measurement errors of up to 25%. However, experimental studies demonstrate that accurate linear measurements can be taken from CT scans if the appropriate scanning and measuring techniques are used (Spoor & Zonneveld, 1991; Spoor et al. 1993; Spoor, 1993). This paper describes a method for morphometric assessment of the labyrinthine size and shape applying these techniques, defines a set of linear and angular measurements for this purpose and evaluates the accuracy by comparing the measurements taken from CT scans with those taken from subsequently made casts and cryosections. The repeatability of the measurements and the number of scans required to obtain a given level of accuracy will also be discussed.

MATERIALS AND METHODS

Specimens

Both temporal bones of 2 dry human skulls and the right temporal bone of a crab-eating macaque (*Macaca fascicularis*, including fresh soft tissue) were scanned. Subsequently, the macaque labyrinth and 3 of the human labyrinths were successfully cast, and used to compare measurements taken from the scans with those taken from the casts. Comparative measurements were also taken from sagittal scans and correlated cryosections of a human and a chimpanzee temporal bone that had been previously prepared for other purposes. Both specimens included soft tissue, the human one unfixed, and the chimpanzee one fixed in ethanol. Finally, to examine the influence of the scanning procedure on the repeatability of the measurements, the right temporal bones of 2 additional dry human skulls were scanned for a second time after 6 months (in the case of one skull) and after an hour (in the case of the other). All specimens were from the collections of the Department of Anatomy of the University of Groningen, The Netherlands, with the exception of the macaque which was obtained from the Rijksinstituut voor Volksgezondheid en Milieuhygiene (RIVM), Bilthoven, The Netherlands.

CT scanning procedure

All CT scans were made on the Philips Tomoscan 350 of the Utrecht University Hospital (The Netherlands) with an exposure of 480 mAs at 120 kVp tube voltage, and the smallest available slice thickness of 1.5 mm to minimise blurring of the imaged structures by partial volume averaging (Zonneveld & Vijverberg, 1984). The gantry was never tilted, as angulation complicates the use of a coordinate system throughout a stack of scans. Zoom reconstructions (matrix 256^2) with a field of view of 80 mm were made using a 'Ramp' convolution filter. In combination with the measuring techniques described below these scanning and reconstruction parameters yield the most accurate linear measurements that can be achieved with the scanner employed in this study (Spoor & Zonneveld, 1991; Spoor, 1993).

Measurements were taken from scans made in the transverse and sagittal plane of the cranium. The transverse plane used in this study intersects the nasion and both poria (i.e. the otoradiological plane defined in Claus et al. (1980) as the 'nasionbiauricular' plane). This plane is approximately parallel to the planar orientation of the lateral semicircular canal, and perpendicular to the planes of the anterior and posterior canals (Zonneveld, 1987), thus facilitating the extraction of a maximum number of significant measurements, including the orientations of the labyrinthine structures to the midsagittal plane of the skull. Sagittal scans reveal essential dimensions which cannot be measured from transverse scans, as well as orientations of labyrinthine structures in the sagittal plane relevant to the ontogenetic and phylogenetic study of the inner ear (Werner 1933, 1960; Saban, 1952; Sercer & Krmpotic, 1958; Delattre & Fenart, 1960, 1961, 1962). As the transverse and sagittal planes are perpendicular to each other, information in one plane can easily be correlated with that in the other.

The specimens that were subsequently cast, were scanned with overlapping slices (slice increment 0.75 mm), which takes approximately 20 transverse and 20 sagittal scans to cover the entire human labyrinth. Examples from both such series are given in Figures 1 and 2 respectively. The 2 human specimens that were used to examine the repeatability were contiguously scanned (slice increment 1.5 mm), with an additional overlapping transverse slice at the level of the lateral semicircular canal (for reasons discussed below). The cryosectioned human and chimpanzee specimens had been previously scanned in frozen condition with contiguous sagittal slices.

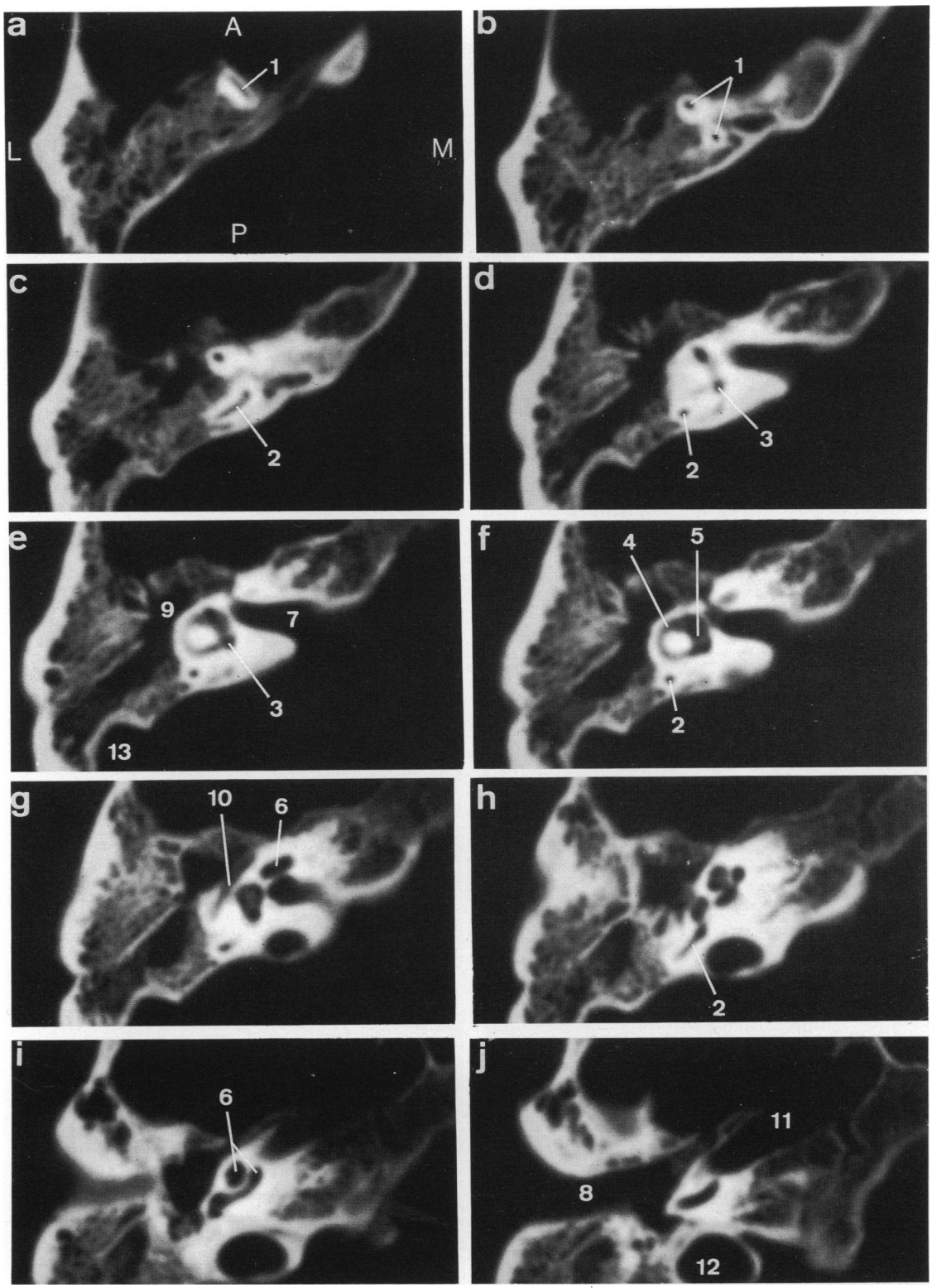

Fig. 1. Transverse CT scans of the temporal bone of a dry human skull going from superior to inferior, showing the labyrinth from the superior tip of the anterior semicircular canal (*a*: 1) to the basal turn of the cochlea (*j*). All scans are made contiguously, except (*e*) which is overlapping with (*d*) and (*f*). A, anterior; P, posterior; L, lateral; M, medial. 1, anterior semicircular canal; 2, posterior semicircular canal; 3, common crus; 4, lateral semicircular canal; 5, vestibule; 6, cochlea; 7, internal acoustic meatus; 8, external acoustic meatus; 9, tympanic cavity; 10, facial canal; 11, carotid canal; 12, jugular fossa; 13, sulcus for sigmoid sinus.

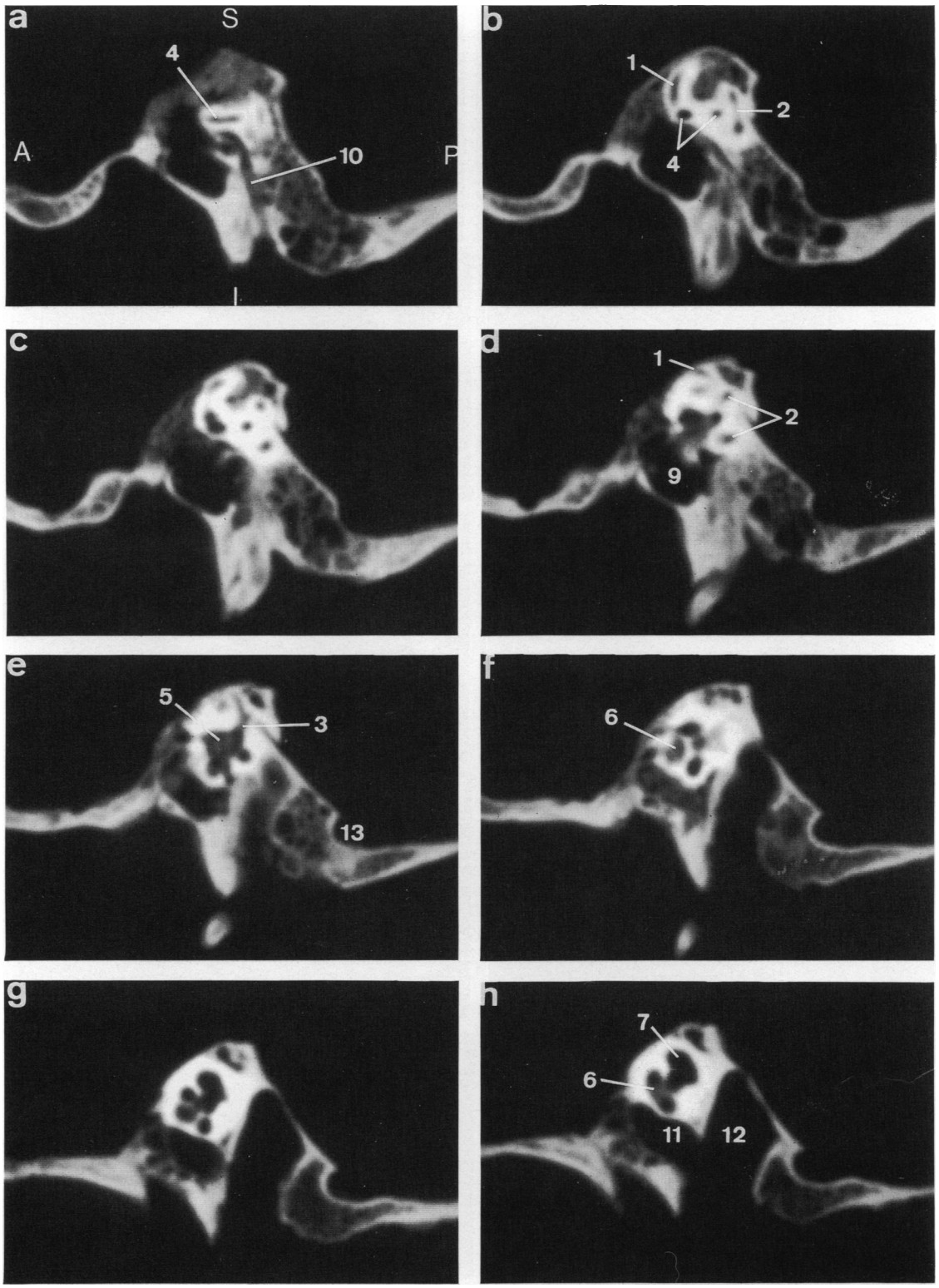

Fig. 2. Contiguous sagittal CT scans of the temporal bone of a dry human skull going from lateral to medial, showing the labyrinth from the lateral tip of the lateral semicircular canal (*a*: 4) to the basal turn of the cochlea (*h*: 6). S, superior; I, inferior; A, anterior; P, posterior. 1, anterior semicircular canal; 2, posterior semicircular canal; 3, common crus; 4, lateral semicircular canal; 5, vestibule; 6, cochlea; 7, internal acoustic meatus; 9, tympanic cavity; 10, facial canal; 11, carotid canal; 12, jugular fossa; 13, sulcus for sigmoid sinus.

Table 1. *The measurements used in this study in alphabetical order of their abbreviation**

APA	Sagittal orientation of the ampullar line of the anterior and posterior semicircular canals (Fig. 3*d*)
ASCh	Height of the anterior semicircular canal (Fig. 3*b*)
ASCm	Transverse orientation of the arc of the anterior semicircular canal (Fig. 3*c*)
ASCs	Transverse orientation of the most superior part of the anterior semicircular canal (Fig. 3*c*)
ASCw	Width of the anterior semicircular canal (Fig. 3*c*)
CC	Transverse orientation of the petrous part of the carotid canal (Fig. 5*m*)
CCR	Sagittal orientation of the common crus (Fig. 3*d*)
COh	Height of the cochlea (Fig. 3*b*)
COs	Sagittal orientation of the cochlea (Fig. 3*d*)
COt	Transverse orientation of the cochlea (Fig. 3*c*)
COw	Width of the cochlea (Fig. 3*a*)
FC2	Transverse orientation of the second part of the facial canal (Fig. 5*n*)
FC3	Sagittal orientation of the third part of the facial canal (Fig. 5*o*)
LSCh	Height of the lateral semicircular canal (Fig. 3*a*)
LSCl	Sagittal orientation of the most lateral part of the lateral semicircular canal (Fig. 3*d*)
LSCm	Sagittal orientation of the arc of the lateral semicircular canal (Fig. 3*d*)
LSCt	Transverse orientation of the central axis of the lateral semicircular canal (Fig. 3*c*)
LSCw	Width of the lateral semicircular canal (Fig. 3*a*)
PPa	Sagittal orientation of the anterior petrosal surface (Fig. 5*r*)
PPp	Sagittal orientation of the posterior petrosal surface (Fig. 5*r*)
PPip	Transverse orientation of the posterior petrosal surface at inferior level (Fig. 5*q*)
PPsp	Transverse orientation of the posterior petrosal surface at superior level (Fig. 5*p*)
PSCh	Height of the posterior semicircular canal (Fig. 3*a*)
PSCi	Transverse orientation of the inferior limb of the posterior semicircular canal (Fig. 3*c*)
PSCm	Transverse orientation of the arc of the posterior semicircular canal (Fig. 3*c*)
PSCs	Transverse orientation of the superior limb of the posterior semicircular canal (Fig. 3*c*)
PSCw	Width of the posterior semicircular canal (Fig. 3*b*)
SLI	Sagittal labyrinthine index (Fig. 3*b*)
TLI	Transverse labyrinthine index (Fig. 3*a*)
V	Transverse orientation of the vestibule (Fig. 3*c*)
VC	Sagittal orientation of the vestibulocochlear line (Fig. 3*d*)

* The full description is given in Appendix 1. Orientations defined in the transverse and the sagittal planes are referred to as transverse and sagittal orientations respectively.

CT measuring procedure

The measurements used in this study, described in detail in the Appendix, consist of 8 dimensions, 14 orientations and 2 indices of the labyrinth, as well as 7 orientations of the carotid canal, the facial canal and the endocranial surface of the petrous pyramid. The measurements are referred to in the text by abbreviations listed in Table 1, and those of the labyrinth are shown in Figure 3.

The dimensions comprise the height and width of the arcs of the semicircular canals and of the basal turn of the cochlea. Among the orientations some describe the planes of the semicircular canals, whereas others concern aspects of the labyrinth and the petrous pyramid described in comparative morphological studies (see Appendix for details). The indices are defined for comparative purposes as well.

The orientations are registered by measuring the angle to the grid of the scan matrix, and any angle between two such orientations can be calculated from these measurements. All orientations are defined in the transverse or sagittal plane, and these angles are therefore projected onto either of these planes. In this study all orientations of the structures in the transverse plane were expressed as angles to the vestibular orientation (Table 1 and Appendix: V) and those in the sagittal plane as angles to the lateral semicircular canal orientation (idem: LSCm). However, as only the differences between CT, cast and section measurements are considered in this study, and not the absolute values, the choice of the reference orientations has no particular importance here.

The landmarks of the measurements are either defined on the boundary of a structure (e.g. on the wall of the vestibule), or in the centre of a lumen (of the semicircular canals and the cochlea). Taking measurements from CT scans by intuitively positioning the measurement points introduces errors because the imaged structures have inevitably blurred boundaries. The method employed in this study therefore uses the CT numbers of the image to determine the exact position of the landmarks. A CT number is the value (in Hounsfield units) assigned to each pixel (picture element) expressing the local X-ray attenuation in the slice of the scanned object, and in a

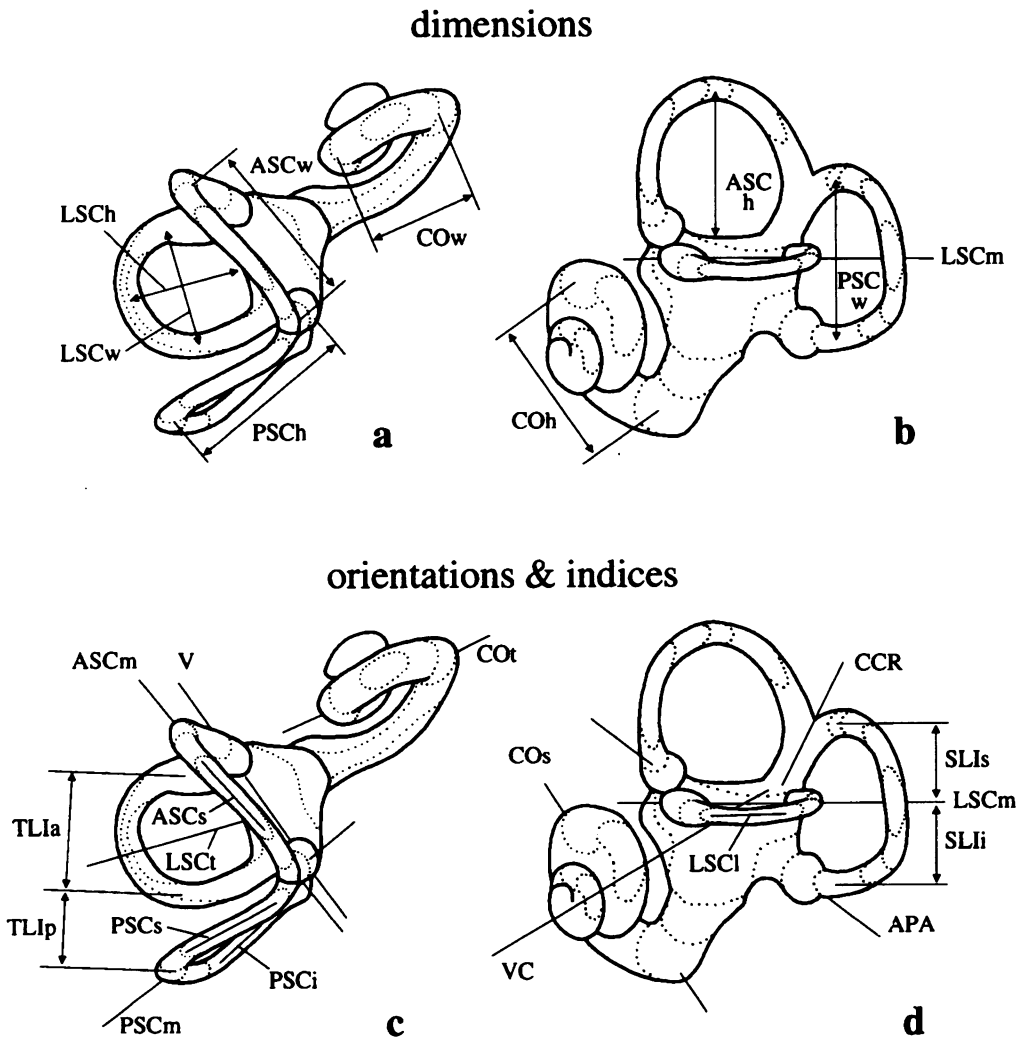

Fig. 3. Superior (*a*, *c*) and lateral (*b*, *d*) aspects of a left human labyrinth, as reconstructed from the CT scans of Figure 1 and 2 respectively, showing the measurements used in this study. Measurement abbreviations are listed in Table 1 and the Appendix. The dotted lines represent the outlines of the labyrinth that appear in individual scans.

CT image these numbers are selectively translated into the grey levels shown on the video screen (regulated by the window width and window level of the console).

At the boundary of a structure, or more generally speaking at any tissue interface, the CT numbers change from the level of one tissue to that of another, but this change is gradual rather than abrupt owing to the limited spatial resolution (see for example Fig. 4*a*: vestibular bone–air interface). In studies based on phantoms as well as extant and fossil bone it has been shown that the interface is located exactly halfway between the 2 CT number levels (Ulrich et al. 1980; Baxter & Sorenson, 1981; Seibert et al. 1981; Spoor et al. 1993). This level, known as half maximum height (HMH), equals the mean of the 2 CT number levels at either side of the interface. By thresholding for the HMH CT number, a technique performed by setting the window width of the viewing console on 1 H(ounsfield) and the window level at the calculated HMH CT number, the position of the interface is visualised as a black–white transition and the measurement point can be placed exactly on the appropriate pixel (i.e. consistently on one side of the black–white transition). This procedure is demonstrated in Figure 4*a* to *c* for the wall of the vestibule.

When the distance between two tissue interfaces is less than twice the spatial resolution of the scan (twice 0.6 mm in this study) the position of neither interface can be determined accurately, owing to effects of interference (Spoor, 1993; Spoor et al. 1993). Measurements taken from casts (Berg, 1903; Gray, 1907; Muren et al. 1986) and serial sections (Curthoys et al. 1977*b*; Igarishi et al. 1981; Ramprashad et al. 1984; Matano et al. 1985, 1986) reveal that the lumen of the semicircular canals of humans, and especially other primates, is frequently smaller than 1.2 mm, and measurements with landmarks defined on the walls of the canals will therefore be prone to inaccurate results.

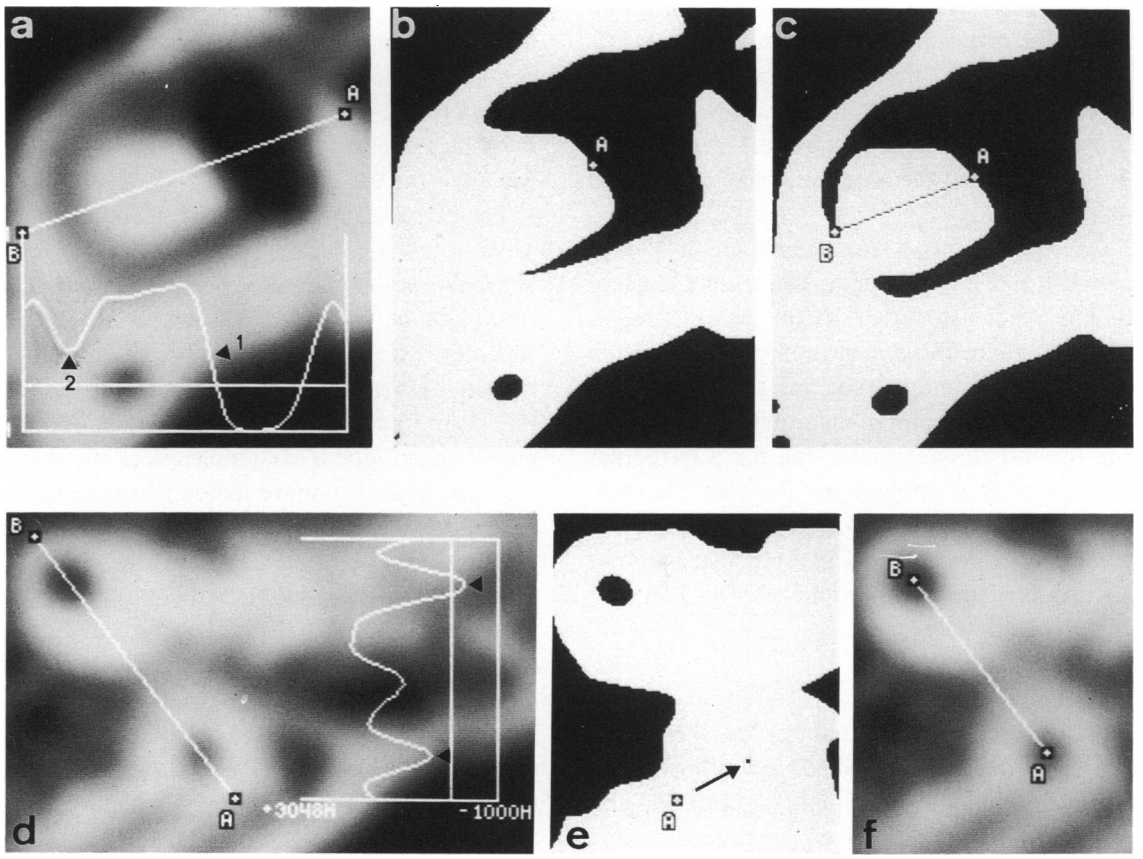

Fig. 4. Method of taking the labyrinthine measurements from CT scans. See text for a detailed description of the procedures.

(*a–c*) Transverse scan of an air-filled human labyrinth (comparable to Fig. 1*f*), showing the process of taking the height of the lateral semicircular canal (LSCh). (*a*) A line A–B is drawn through the estimated position of the landmarks on the vestibular wall and in the lumen of the lateral semicircular canal. The graph of the CT numbers along line A–B shows the gradual change from bone (2080 H) to air (−1000 H) at the wall of the vestibule. Arrowhead 1 indicates the half maximum height (HMH) value (540 H) of this CT number transition representing the true position of the vestibular wall. The graph also shows that the CT numbers in the air-filled lateral semicircular canal do not reach the true value of air. Arrowhead 2 points at the minimum CT number (701 H) indicating the pixel in the centre of the canal (window level (WL) 1000 H, window width (WW) 4095 H). (*b*) The true position of the vestibular wall is visualised by thresholding for the local HMH value (WL 540 H, WW 1 H), and measurement point A is placed. (*c*) The centre of the canal is visualised by thresholding for the local minimum CT number (WL 701 H, WW 1 H), measurement point B is placed, and the height of the lateral semicircular canal (A − B) thus is obtained.

(*d–f*) Transverse scan of an air-filled human labyrinth (comparable to Fig. 1*c*), showing the process of taking the width of the anterior semicircular canal (ASCw). (*d*) The CT number graph of line A–B through the 2 sections of the anterior semicircular canal demonstrates that the CT numbers in both lumina do not reach the value of air. The minimum CT numbers (arrowheads) pertain to the pixel in the centre of each lumen (WL 1000 H, WW 4095 H). (*e*) By thresholding for the minimum CT number of one of the lumina its centre is visualised by a single pixel and measurement point A can be placed (WL 419, WW 1). (*f*) This procedure is repeated for the other lumen and after placing measurement point B the centre to centre width of the anterior semicircular canal is obtained (WL 1000 H, WW 4095 H).

Hence, diameter measurements of the lumen of the semicircular canals or the cochlea are not included in this study. Regarding linear measurements of the arc of the semicircular canals or the basal turn of the cochlea, the possible error introduced by using landmarks on the lumen wall is less significant (if expressed as a percentage of the true value). However, the results of phantom studies suggest that measurements with landmarks in the centre of small lumina potentially give very accurate results (Spoor & Zonneveld, 1991; Spoor, 1993), and therefore all dimensions used in this study are defined accordingly.

The CT numbers of air-filled or liquid-filled lumina of the semicircular canals and the cochlea do not reach the true value of air (−1000 H) or liquid (about 0 H), owing to the same interference effect that hampers diameter measurements of the lumen. CT number profiles of such lumina show a distinct minimum (Fig. 4*a*, *d*; arrowheads), and the pixel with this minimum CT number is located exactly in the centre of the lumen (Spoor & Zonneveld, 1991; Spoor, 1993). The central pixel can be visualised by thresholding at the minimum CT number. In practice this can be done by using a window width of 1 H and

experimentally lowering the window level until only a single pixel (the one with the minimum CT number) is shown. Subsequently, the measurement point can exactly be placed on this central pixel. This procedure is demonstrated for sections of the lateral semicircular canal (Fig. 4*a–c*), and the anterior semicircular canal (Fig. 4*d–f*).

The CT measurements were made on a Philips SAVC or LX viewing console to the nearest tenth of a millimetre (dimensions) or to the nearest degree (angles). The labyrinthine measurements were taken from $\times 4$ magnified images reducing the pixel size of 0.3 mm to less than the unit of measurement (0.1 mm). Selecting the most appropriate scan for a particular measurement was simplified by drawing the labyrinthine contours of each scan on the screen of the viewing console, thus building up a reconstruction of the labyrinth (see the contours indicated in Fig. 3).

Casting and sectioning

The human and macaque labyrinths were cast following the method described by Wilbrand & Rauschning (1986). After thoroughly macerating and degreasing the isolated petrous pyramids, using trypsin and acetone, the intraosseous spaces were filled under vacuum with the plastic Technovit 3040 (maximum volumetric shrinkage of 6.1%). All bone tissue was subsequently removed from the plastic cast using hydrochloric acid, and structures other than the bony labyrinth were removed using a dental drill.

Most of the landmarks are located inside the cast, e.g. in the centre of the canals, and therefore the measurements taken from the casts are derived from the external dimensions and surface curvatures. The dimensions were measured to the nearest tenth of a millimetre, using a Leitz Orthoplan FSA-GW (Germany) measuring microscope. The actual heights and widths of the semicircular canals and the cochlea were taken from the casts, whereas the equivalent measurements taken from the CT scans are dimensions projected on to the transverse or sagittal plane (but with the aim to approximate the actual 'nonprojected' size). Hence comparison of the CT and casts measurements not only assesses the accuracy of the CT technique, but also the possible error introduced by the projection of the dimension.

The orientations were recorded to the nearest degree, using 2 sharp pointers to bring a measuring device in line with the relevant labyrinthine structure. The orientations and index defined in the transverse plane were taken parallel to the planar orientation of the lateral semicircular canal. Those defined in the sagittal plane were taken in a plane as close as possible to the original sagittal scan plane (estimated by comparing the cast with the labyrinthine reconstruction on the basis of the sagittal scans (e.g. Fig. 3*b*, *d*)). Each measurement was made 3 times, and the mean was used for the comparison.

The orientation of the vestibulocochlear line (VC) was not included in the scan-cast comparison, as the vestibular landmark (see Appendix for the definition) could not be registered on the casts with sufficient accuracy. Measurements PSCw,i, COw, and SLI of 1 human labyrinth, and measurements ASCh,s, PSCh,s,m,i and TLI of the macaque labyrinth could not be taken, due to incompleteness of the casts.

It was generally more difficult to take the angular measurements defined in the sagittal scans from the casts than those defined in the transverse scans. Hence, to obtain additional information on the measurements in the sagittal plane, comparison was made between correlated CT scans and cryosections of a human and a chimpanzee temporal bone that had been previously prepared for other purposes. In the procedure, described in detail in Zonneveld (1987), the tissue blocks had been embedded in frozen carboxy-methyl cellulose (CMC) gel, and sectioned in the sagittal plane on an LKB 2250 cryomicrotome (Department of Anatomy, University of Groningen) with a slice thickness of 0.02 mm. The cryosectional surface had been photographed every 0.16 mm (135 mm macro objective, Kodak EN 100 slide film), thus providing almost 10 times as many images as in CT to make the sagittal labyrinthine measurements.

Data analysis

In addition to the comparison of measurements taken from the CT scans, the casts and the sections, the influence of the CT slice increment on the accuracy of the measurements was studied. If the slice increment between the scans is increased the measurements become less accurate, as the number of 'samples' taken from the labyrinth is reduced, an effect studied here using the overlapping scans of the specimens that were cast (4 human labyrinths and 1 macaque labyrinth). Each stack of overlapping slices was split into 2 new series of contiguous slices, and the differences between the measurements taken from each contiguous series and the total stack represent the errors that occur when the slice increment is increased from 0.75 to 1.5 mm.

Most of the labyrinthine measurements use landmarks that are virtually 100% reproducible in a given series of scans, as they are based on thresholding for

a single central pixel, or for the HMH value of an interface. However, the orientations of the lateral semicircular canal in the transverse plane (LSCt) and the common crus in the sagittal plane (CCR) are partly determined subjectively. To assess the intra-observer variation, both measurements were repeated 5 times for 10 labyrinths over a period of 3 months by the first author, who had extensive experience with the method of measuring. To assess the intraobserver variation, the orientations were measured once by the second author who was at the time not familiar with taking these measurements.

RESULTS

The differences between the measurements taken from the casts and the scans and from the cryosections and the scans are listed in Tables 2 and 3 respectively. In both tables the results obtained for the human and nonhuman labyrinths are combined as they are not significantly different.

The differences between the measurements taken from series of contiguous and overlapping scans of the human labyrinths are listed in Table 4. The doubled slice increment results in marked underestimation of the height of the posterior canal (PSCh) by up to 0.8 mm, as the location of the landmark in the common crus is sensitive to changes in slice position. In addition, both dimensions of the cochlea (COh,w) are sometimes underestimated by 0.2 mm, an error also observed in the comparison between the cryosections and the contiguous scans (Table 3). For the orientations and the indices of the human labyrinth the errors introduced by doubling the slice increment are small and comparable to the differences observed between the scans and the casts.

Eight measurements of the macaque labyrinth (LSCh,w,t,l, ASCs, PSCs,i and TLI) could only be taken from single scans of the overlapping series because the lumina of its semicircular canals are markedly smaller than those of the human and chimpanzee labyrinths. Full comparison between the measurements taken from series of contiguous and overlapping scans is therefore not possible. The differences between the measurements that can be taken from both series, fall within the ranges observed for the human labyrinth (Table 4).

The differences between the measurements taken from the original and from the repeated series of scans are listed in Table 5, and the intraobserver and inter-observer variation measured for the orientations of the lateral semicircular canal and the common crus are given in Table 6.

Table 2. *Differences between measurements of 4 labyrinths (3 human, 1 macaque) taken from overlapping CT scans and from casts (CT-value minus cast-value)**

	Angles	Dimensions	Indices
n	39	28	6
mean	0.2	0.00	0.2
min	−3	−0.1	−2 (SLI)
max	4	0.1	1
S.D.	2.1	0.06	1.1

* n, number of comparisons made. The angles are given in degrees, dimensions in millimetres and indices in percentages. If minimum or maximum differences are caused by a single type of measurement its abbreviation is given in parentheses.

Table 3. *Differences between measurements of 2 labyrinths (1 human, 1 chimpanzee) taken from contiguous sagittal scans and from cryosections (CT-value minus cryosection value)**

	Angles	Dimensions	Index (SLI)
n	10	6	2
mean	−0.1	−0.05	0.5
min	−3 (VC)	−0.2 (COh)	−1
max	3 (VC)	0.0	2
S.D.	1.8	0.09	1.5

* Presentation similar to Table 2.

Table 4. *Differences between measurements taken from 2 series of contiguous scans and from combined stack of overlapping scans for 4 human petrous bones (contiguous-value minus overlapping-value)**

	Angles lab	Angles lab+petr	Dimensions	Indices
n	104	160	64	16
mean	0.0	0.0	−0.05	−0.1
min	−4	−4	−0.8 (PSCh)	−3 (SLI)
max	3	3	0.1 (LSCh)	2 (SLI)
S.D.	1.3	1.1	0.15	1.2

* Presentation as in Table 2. lab, angles of labyrinth only; petr, angles of the facial and carotid canal and the petrous pyramid.

Table 5. *Absolute differences between measurements taken from an original and a repeated series of scans of 2 human temporal bones**

	Angles lab	Angles lab+petr	Dimensions	Indices
n	26	40	16	4
mean	0.8	0.9	0.02	1.1
min	0	0	0.0	0
max	2	2	0.1	2 (SLI)
S.D.	0.6	0.7	0.04	0.7

* Presentation as in Table 2.

Table 6. *Intraobserver and interobserver variation of measuring the orientation of the central axis of the lateral semicircular canal in the transverse plane (LSCt) and the orientation of the common crus in the sagittal plane (CCR) for 10 human labyrinths**

	LSCt		CCR	
	Intra-observer	Inter-observer	Intra-observer	Inter-observer
n	50	10	50	10
mean	0.9	−2.7	0.8	1.8
min	0	−7	0	−3
max	3	5	3	6
S.D.	0.7	3.3	0.6	2.1

* Intraobserver: the absolute difference between 5 repeated measurements and their mean. Interobserver: the difference between the mean of the 5 measurements taken by the first observer and the measurement taken by the second observer.

DISCUSSION

The differences between the measurements obtained from the casts or cryosections and the CT scans do not necessarily represent errors of the CT method. Measurements taken from the casts may have been influenced by shrinkage during the solidification process. However, the maximum volumetric shrinkage of 6.1% of the casting material will result in a linear shrinkage of 1.8%, and for surface landmarks on small structures such as the semicircular canals this will hardly affect measurements taken to the nearest tenth of a millimetre, or nearest degree. Moreover, small shrinkage errors of surface landmarks are cancelled out when calculating the landmarks in the centre of a structure. Small errors may be introduced when estimating the internal landmarks from the external cast surface is not totally unambiguous, as was mainly the case for the cochlear dimensions and orientations. Part of the observed differences between the cryosections and the scans may be caused by small discrepancies in the alignment of the planes of scanning and sectioning. Bearing these caveats in mind, the largest differences of ±0.1 mm, ±4° and ±2% observed for the dimensions, orientations and indices, respectively, are likely to be reasonable estimates of the maximum error ranges of the CT-based method.

The maximum errors of ±0.1 mm equal the best possible accuracy of linear measurements that can be achieved with the scanner employed in this study (Spoor & Zonneveld, 1991; Spoor, 1993; Spoor et al. 1993). The 0.1 mm corresponds to relative errors of 3% (human, chimpanzee) and 5% (macaque) for the dimensions of the cochlea and 2% (human, chimpanzee) and 3% (macaque) for those of the semicircular canals. The latter are far smaller than the errors of up to 25% obtained by Muren & Ytterbergh (1986) for the dimensions of the semicircular canals. The most probable reason for their inaccurate results may be that their CT landmarks are defined on the walls of the canals, which introduces measurement errors owing to the effects of interference of the two boundaries (Spoor, 1993; Spoor et al. 1993).

The method of determining the centre of a labyrinthine lumen via the pixel with the minimum CT number theoretically requires a homogeneous content of the lumen. However, the similar results obtained for the liquid and air-filled labyrinths indicate that the presence of the membranous labyrinth inside the bony semicircular canals does not reduce the accuracy of the measurements (owing to partial volume averaging with the surrounding liquid). Likewise, the thin bony spiral lamina of the cochlea is not clearly visualised in the CT sections in which the measurements are made, and it may have only minor influence on the central position of the measurement point.

The use of contiguous instead of overlapping slices halves the number of scans required for each labyrinth and thus reduces the resources required. For the macaque labyrinth this is not possible because virtually a full stack of overlapping scans must be made to obtain all images required for the measurements. For the human labyrinth doubling the slice increment introduces significant errors (Table 4), and therefore a combination of contiguous and overlapping slices might give the best results if both accuracy and a minimum number of scans are required. The largest errors in contiguous scans, observed for the height of the posterior semicircular canal (PSCh), can be eliminated by adding an overlapping transverse scan at the level of the lateral semicircular canal (e.g. Fig. 1*e* between 1*d* and 1*f*). This has the advantage that the accuracy of 7 other measurements (LSCh,w,t, V, PSCm, PPip and TLI) is also optimised. The reduced range of dimensional errors after adding this overlapping scan is shown in Table 7. The maximum errors of −0.2 mm thus obtained for the cochlear dimensions can be avoided by adding a transverse and a sagittal overlapping scan at the appropriate level, but the occurrence of these errors may be considered acceptable because, relative to the cochlear dimensions, they do not exceed the 5% level.

The combination of contiguous scans plus one overlapping transverse slice at the level of the lateral semicircular canal was used when testing the precision (repeatability) of the CT-based measurements. The

Table 7. *Comparison of measurements taken from contiguous and overlapping scans similar to Table 4, but after adding one overlapping transverse scan at the level of the lateral semicircular canal in each transverse contiguous series*

	Angles lab	Angles lab+petr	Dimensions	Indices
n	104	160	64	16
mean	0.0	0.0	−0.02	0.1
min	−4 (COt)	−4 (COt)	−0.2 (COh,w)	−3 (SLI)
max	3	3	0.0	2 (SLI)
S.D.	1.0	0.9	0.06	0.9

differences between the measurements taken from the original and the repeated series of scans are small (Table 5) and do not exceed those between the scans and the casts or cryosections (Tables 2, 3), suggesting that placing the skull in the correct plane in the scanner and making the scans is a reproducible procedure that does not introduce major errors.

Concerning the intraobserver variation of measuring LSCt and CCR the average deviation of the mean of just 1° indicates that both measurements are reproducible (Table 6), despite the fact that there might be a subjective factor involved in taking these measurements. The average intraobserver deviation of LSCt and CCR is only 2°–3°, and the pattern of both positive and negative deviations suggests the absence of systematic differences in the assessment of the orientations by the two observers (Table 6). The relatively large ranges of interobserver variation, if compared with those of the intraobserver variation, are most probably the consequence of the lack of experience of the second observer with taking these measurements.

CONCLUSIONS

In conclusion this study demonstrates that measurements of the 8 dimensions, 14 orientations and 2 indices describing the size and shape of the bony labyrinth can be taken from overlapping transverse and sagittal CT scans with an accuracy and precision that correspond to maximum errors of ±0.1 mm, ±4° and ±2%, respectively. The practical significance of these errors may be considered relative to the morphological variation of the labyrinthine structures. The width of the arc of the anterior, lateral and posterior semicircular canals, measured on 95 cast labyrinths from a single human population, varies by 2.1, 2.4 and 3.3 mm respectively (based on the raw data of Muren et al. 1986), and the cochlear dimensions of these casts vary by 1.5 to 2.8 mm (Dimopoulos & Muren, 1990). Measurements of cast human labyrinths reveal that the angles between the planes of the semicircular canals vary by ~ 30° (Sato, 1903; Schönemann, 1906). The human labyrinth is not unique in this respect, as the planar orientation and the dimensions of the semicircular canals in cat, guinea pig and humans show similar levels of variation (Blanks et al. 1972, 1975; Curthoys et al. 1975, 1977*a*). Given these levels of variation, it is concluded that the method presented in this study is sufficiently accurate to be used for the morphometric analysis of the primate bony labyrinth.

As CT allows for the nondestructive study of skulls in anthropological and primatological museum collections it holds out the prospect that little-known aspects of the human labyrinth, such as morphological variation, ontogenetic trends, and its comparative relationship to the labyrinth of other primates, can be evaluated. Moreover, the evolutionary history of the human labyrinth can be investigated as CT visualises the bony labyrinth in fossil hominid skulls (Zonneveld & Wind, 1985; Zonneveld et al. 1989), and fossilisation per se does not diminish the accuracy of CT-based measurements (Spoor et al. 1993). Such analyses will also provide metrical data for the labyrinth that may be used in efforts to understand the functional morphology of the vestibular system, and to test models of hydrodynamic endolymph movement (Jones & Spells, 1963; Ten Kate et al. 1970; Oman et al. 1987; Muller & Verhagen, 1988*a*, *b*; Muller, 1990). The first results of a CT-based analysis along these lines are reported in Spoor et al. (1994), a comparative study discussing the semicircular canal dimensions in humans and their fossil ancestors. Finally, the quantitative evaluation of labyrinthine morphology in vivo may aid in the diagnosis of inner ear pathology (De Groot, 1987; Pappas et al. 1990; Dimopoulos & Muren, 1990).

ACKNOWLEDGEMENTS

We thank Mr A. Timmerman and Professor G. N. Van Vark for providing the specimens, Dr P. Gerrits, Mr H. Horlings, Ms B. Van Leeuwen and Mr J. Legrand for their help with the preparation of cryosections and casts of the temporal bones and Mr J. De Groot and Mr M. Metselaar for carrying out the CT photography. We are grateful to Professor B. Wood, Dr A. Turner, Professor G. N. Van Vark and 2 anonymous referees for critically reviewing the manuscript and to the Universities of Groningen and Liverpool and Philips Medical Systems for their support.

REFERENCES

BAXTER BS, SORENSON JA (1981) Factors affecting the measurement of size and CT number in computed tomography. *Investigative Radiology* **16**, 337–341.

BERG W (1903) Zur Corrosionanatomie des Schläfenbein der Affen. *Zeitschrift für Morphologie und Anthropologie* **5**, 315–345.

BLANKS RHI, CURTHOYS IS, MARKHAM CH (1972) Planar relationships of the semicircular canals in the cat. *American Journal of Physiology* **223**, 55–62.

BLANKS RHI, CURTHOYS IS, MARKHAM CH (1975) Planar relationships of the semicircular canals in man. *Acta Otolaryngologica* **80**, 185–196.

BLANKS RHI, CURTHOYS IS, BENNETT ML, MARKHAM CH (1985) Planar relationship of the semicircular canals in rhesus and squirrel monkeys. *Brain Research* **340**, 315–324.

CAIX M, OUTREQUIN G (1976) Les canaux semi-circulaires. *Monographie du College Medical Français des Professeurs d'Anatomie.*

CAIX M, OUTREQUIN G (1979) Variability of the bony semicircular canals. *Anatomia Clinica* **1**, 259–265.

CLAUS E, LEMAHIEU SF, ERNOULD D (1980) The most used otoradiological projections. *Journal Belgique de Radiologie* **63**, 1838–203.

CURTHOYS IS, CURTHOYS EJ, BLANKS RHI, MARKHAM CH (1975) The orientation of the semicircular canals in the guinea pig. *Acta Otolaryngologica* **80**, 197–205.

CURTHOYS IS, BLANKS RHI, MARKHAM CH (1977*a*) Semicircular canal radii of curvature (R) in cat, guinea pig and man. *Journal of Morphology* **151**, 1–16.

CURTHOYS IS, MARKHAM CH, CURTHOYS EJ (1977*b*) Semicircular duct and ampulla dimensions in cat, guinea pig and man. *Journal of Morphology* **151**, 17–34.

DE GROOT JAM (1987) *Computed tomography of the petrous bone in otosclerosis and Ménière's disease.* Doctoral thesis, University of Utrecht, The Netherlands.

DELATTRE A (1951) La rotation vestibulaire. *Comptes Rendus des Séances de l'Academie des Sciences* **233**, 978–980.

DELATTRE A, FENART R (1960) *L'Hominisation de Crâne Etudiée par la Methode Vestibulaire.* Paris: CNRS.

DELATTRE A, FENART R (1961) Evolution des fenêtres du vestibule des mammifères a l'homme. *Bulletins de la Societé d'Anthropologie* **T2, Sér. XI**, 273–289.

DELATTRE A, FENART R (1962) Formation des orfices de la face postérieure du rocher humain. *Mammalia* **26**, 214–279.

DENKER A (1899) *Vergleichend-anatomische Untersuchungen über das Gehörorgan der Säugethiere nach Corrosionspräparaten und Knochenschnitten.* Leipzig: Von Veit and Co.

DIMOPOULOS P, MUREN C (1990) Anatomic variations of the cochlea and relations to other temporal bone structures. *Acta Radiologica, Diagnosis* **31**, 439–444.

FENART R, DEBLOCK R (1973) *Pan paniscus* et *Pan troglodytes* craniometrie. *Annales de la Musée Royal de l'Afrique Centrale, Tervuren, Belgique*, **Sér. IN-8**, 1–204.

FENART R, PELLERIN C (1988) The vestibular orientation method; its application in the determination of an average human skull type. *International Journal of Anthropology* **3**, 223–219.

GIRARD L (1923) Le plan des canaux semi-circulaires horizontaux consideré comme plan horizontal de la tête. *Bulletins et Mémoirs de la Societé d'Anthropologie de Paris* **7**, 14–33.

GIRARD L (1947) Port habituel de la tête et fonction vestibulaire. *Mammalia* **11**, 1–17.

GRAY AA (1907) *The Labyrinth of Animals.* London: Churchill.

HYRTL J (1845) *Vergleichend-anatomische Untersuchungen über das innere Gehörorgan des Menschen und der Säugethiere*, vol. 3. Prague: F. Ehrlich.

IGARASHI M (1967) Dimensional study of the vestibular apparatus. *Laryngoscope* **77**, 1806–1817.

IGARASHI M, O-UCHI T, ALFORD BR (1981) Volumetric and dimensional measurements of vestibular structures in the squirrel monkey. *Acta Otolaryngologica* **91**, 437–444.

JONES GM, SPELLS KE (1963) A theoretical and comparative study of the functional dependence of the semicircular canal upon its physical dimensions. *Proceedings of the Royal Society, London* **B 157**, 403–419.

LEBEDKIN S (1924) Über die Lage des Canalis semicircularis lateralis bei Säugern. *Anatomischer Anzeiger* **58**, 447–460.

MATANO S, KUBO T, GÜNTHER M (1985) Semicircular canal organ in three primate species and behavioural correlations. *Fortschritte der Zoologie* **30**, 677–680.

MATANO S, KUBO T, MATSUNAGA T, NIEMITZ C, GÜNTHER M (1986) On the size of the semicircular canals organ in the *Tarsius bancanus.* In *Current Perspectives in Primate Biology* (ed. D. M. Taub & F. A. King), pp. 122–129. New York: Van Nostrand Reinhold.

MULLER M (1990) Relationship between semicircular duct radii with some implications for time constants. *Netherlands Journal of Zoology* **40**, 173–202.

MULLER M, VERHAGEN JHG (1988*a*) A new quantitative model of total endolymph flow in the system of semicircular ducts. *Journal of Theoretical Biology* **134**, 473–501.

MULLER M, VERHAGEN JHG (1988*b*) A mathematical approach enabling the calculation of the total endolymph flow in the semicircular ducts. *Journal of Theoretical Biology* **134**, 503–529.

MUREN C, YTTERBERGH C (1986) Computed tomography of temporal bone specimens. A test of the resolution capability. *Acta Radiologica, Diagnosis* **27**, 645–651.

MUREN C, RUHN G, WILBRAND H (1986) Anatomic variations of the human semicircular canals. *Acta Radiologica, Diagnosis* **27**, 157–163.

OMAN CM, MARCUS EN, CURTHOYS IS (1987) The influence of the semicircular canal morphology on endolymph flow dynamics. *Acta Otolaryngologica* **103**, 1–13.

PAPPAS DG, SIMPSON LD, MCKENZIE RA, ROYAL S (1990) High-resolution computed tomography: determination of the cause of pediatric sensorineural hearing loss. *Laryngoscope* **100**, 564–569.

PEREZ F (1922) Craniologie vestibienne, ethnique et zoologique. *Bulletins et Mémoirs de la Societé d'Anthropologie de Paris* **7**, 16–32.

RAMPRASHAD F, LANDOLT JP, MONEY KE, LAUFER J (1984) Dimensional analysis and dynamic response characterization of mammalian peripheral vestibular structures. *American Journal of Anatomy* **169**, 295–313.

REISINE H, SIMPSON JI, HENN V (1988) A geometric analysis of semicircular canals and induced activity in their peripheral afferents in the rhesus monkey. *Annals of the New York Academy of Science* **545**, 10–20.

ROBIN M, CAIX M, OUTREQUIN G (1968) Contribution à l'étude radiologique de l'orientation des plans ampullaires chez l'homme. *Comptes Rendus de l'Association d'Anatomie* **139**, 1056–1071.

SABAN R (1952) Fixité du canal semi-circulaire externe et variations de l'angle thyridien. *Mammalia* **16**, 77–92.

SATO T (1903) Vergleichende Untersuchungen über die bogengänge des Labyrinthes beim neugeborenen und beim erwachsenen Menschen. *Zeitschrift für Ohrenheilkunde* **42**, 137–156.

SCHÖNEMANN A (1906) Schläfenbein und Schädelbasis, eine anatomisch-otiatrische Studie. *Neue Denkschriften der algemeinen Schweizerischen Gesellschaft für die gesamten Naturwissenschaften* **40**, 95–160.

SERCER A, KRMPOTIC J (1958) Further contributions to the development of the labyrinthine capsule. *Journal of Laryngology and Otology* **72**, 688–698.

SICK H, VEILLON F (1988) *Atlas of Slices of the Temporal Bone and Adjacent Region.* München: Bergman Verlag.

SEIBERT CE, BARNES JE, DREISBACH JN, SWANSON WB, HECK RJ (1981) Accurate CT measurement of the spinal cord using metrizimide: physical factors. *American Journal of Radiology* **136**, 777–780.

SIEBENMANN F (1890) *Die Korrosions-Anatomie des knöchernen Labyrinthes des menschlichen Ohres.* Wiesbaden: J. F. Bergmann.

SPOOR CF (1993) *The Comparative Morphology and Phylogeny of the Human Bony Labyrinth.* Doctoral thesis, University of Utrecht, The Netherlands.

SPOOR CF, ZONNEVELD FW (1991) Biometry using computed tomography, a phantom study. *European Journal of Morphology* **29**, 116.

SPOOR CF, ZONNEVELD FW, MACHO GA (1993) Linear measurements of cortical bone and dental enamel by computed tomography: applications and problems. *American Journal of Physical Anthropology* **91**, 469–484.

SPOOR F, WOOD B, ZONNEVELD F (1994) Implications of early hominid labyrinthine morphology for the evolution of human bipedal locomotion. *Nature* **369**, 645–648.

TEN KATE JH, BARNEVELD HH, KUIPER JW (1970) The dimensions and sensitivities of semicircular canals. *Journal of Experimental Biology* **53**, 501–514.

TURKEWITSCH BG (1930) Alters- und Geslechtseigenschaften de anatomischen Baues des menschlichen knöchernen Labyrinthes. *Anatomischer Anzeiger* **70**, 225–234.

ULRICH CG, BINET EF, SANECKI MG, KIEFFER SA (1980) Quantitative assessment of the lumbar spinal canal by computed tomography. *Radiology* **134**, 137–143.

VILLEMIN F, BEAUVIEUX J (1934) Recherche sur la topographie des canaux semi-circulaires et leurs ampoules chez les vertébrés. *Comptes Rendus de la Societé de Biologie de Bordeaux*, 553–555.

WERNER CF (1993) Das Ohrlabyrinth der Tiere. *Passow-Schäfer Beiträge* **30**, 390–408.

WERNER CF (1960) Das Ohr, A. Mittel- und Innenohr. In *Primatologia, Handbuch der Primatenkunde* II.1.5 (ed. H. Hofer, A. H. Schultz & D. Starck), pp. 1–38. Basel: S. Karger.

WILBRAND H, RAUSCHNING W (1986) Investigation of temporal bone anatomy by plastic moulding and cryomicrotomy. *Acta Radiologica, Diagnosis* **27**, 389–394.

ZONNEVELD FW (1987) *Computed Tomography of the Temporal Bone and Orbit.* Munich: Urban and Schwarzenberg.

ZONNEVELD FW, SPOOR CF, WIND J (1989) The use of computed tomography in the study of the internal morphology of hominid fossils. *Medicamundi* **34**, 117–128.

ZONNEVELD FW, VIJVERBERG GP (1984) The relationship between slice thickness and image quality in CT. *Medicamundi* **29**, 104–117.

ZONNEVELD FW, WIND J (1985) High-resolution computed tomography of fossil hominid skulls: a new method and some results. In *Hominid Evolution, Past, Present and Future* (ed. P. V. Tobias), pp. 427–436. New York: Alan Liss.

APPENDIX. DEFINITION OF THE MEASUREMENTS

The definitions of the dimensions, orientations and indices are listed according to the anatomical structure(s) involved, and in Figure 5 the measurements are indicated in relation to line tracings of the CT scans given in Figures 1 and 2.

Labyrinthine dimensions

Following the definitions in previous morphometric studies, the height of the semicircular canals is always the distance between vestibule and the point on the arc furthest from the vestibule, independent of the orientation of this dimension in space, and the width of the arc is taken perpendicular to the height.

ASCh. Height of the arc of the anterior semicircular canal. Measured in the sagittal plane and defined as the distance from the centre of the most superior part of the anterior semicircular canal to the superior wall of the vestibule perpendicular to the orientation of the lateral semicircular canal, defined below as LSCm (Fig. 2*d*, 3 *b*, 5*i*). Occasionally its 2 landmarks do not appear in a single scan, and the x, y pixel coordinates of each landmark must be recorded in the adjacent scans which can be used to calculate the distance projected in the sagittal plane (however, 2 landmarks in a single scan are also projected over the slice thickness of 1.5 mm).

ASCw. Width of the arc of the anterior semicircular canal. Measured in the transverse plane and defined as the largest centre to centre distance between its anterior limb and either its posterior limb or the common crus in this plane (Figs 1*c*, 3*a*, 4*d*, 5*b*).

PSch. Height of the arc of the posterior semicircular canal. Defined as the largest centre to centre distance between the posterior limb of the posterior semicircular canal and the common crus in the transverse plane (Figs 1*e*, 3*a*, 5*c*). The landmark in the common crus usually is located in its aperture into the vestibule.

PSCw. Width of the arc of the posterior semicircular canal. Measured in the sagittal plane and defined as the centre to centre distance between the most superior and most inferior part of the posterior semicircular canal, perpendicular to the orientation of the lateral semicircular canal (LSCm). Occasionally the 2 landmarks are shown in adjacent scans, and a projected distance can be calculated from their pixel coordinates (Figs 2*d*, 3*b*, 5*i*).

LSCh. Height of the arc of the lateral semicircular canal. Measured in the transverse plane from the scan which best displays the complete extent of the canal. It is defined as the distance from the vestibular wall between both limbs of the lateral semicircular canal to the centre of the opposing (lateroposterior) part of the canal. The point on the vestibular wall is equidistant between the apertures of the ampulla and posterior limb of the canal into the vestibule, measured from their centre. The opposing lateroposterior point is defined as the compromise between the two criteria. (1) It has the largest distance from the vestibular point, and (2) the line connecting the 2 landmarks bisects the area enclosed by the arc of the lateral semicircular canal (Fig. 1*f*, 3*a*, 4*a*, 5*d*).

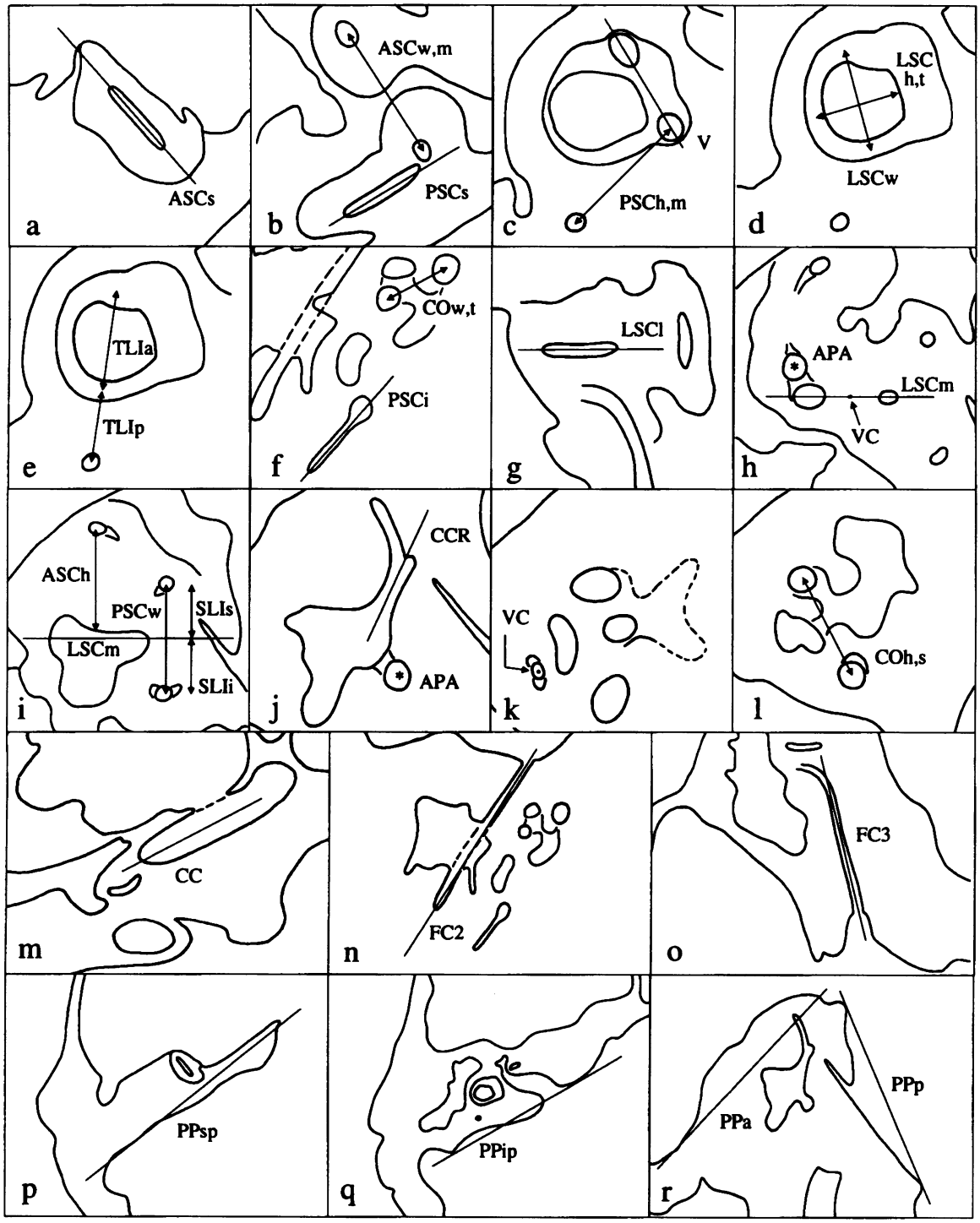

Fig. 5. The dimensions, orientations and indices of the bony labyrinth and the petrous pyramid shown in line tracings of the transverse and sagittal CT scans of Figures 1 and 2. Measurement abbreviations are listed in the Appendix and Table 1. Sources of the line tracings: (*a*) Fig. 1*a*, (*b*) Fig. 1*c*, (*c*) Fig. 1*e*, (*d*) Fig. 1*f*, (*e*) Fig. 1*f*, (*f*) Fig. 1*h*, (*g*) Fig. 2*a*, (*h*) Fig. 2*c*, (*i*) Fig. 2*d*, (*j*) Fig. 2*e*, (*k*) Fig. 2*f*, (*l*) *Fig.* 2*g*, (*m*) Fig. 1*e*, (*n*) Fig. 1*h*, (*o*) Fig. 2*a*, (*p*) Fig. 1*a*, (*q*) Fig. 1*f*, (*r*) Fig. 2*e*.

LSCw. Width of the arc of the lateral semicircular canal. Measured in the transverse plane, usually from the same scan as LSCh. It is defined as the largest centre to centre distance between the anterior and posterior limbs, perpendicular to LSCh (Figs 1*f*, 3*a*, 5*d*).

COh. Height of the basal turn of the cochlea (CO). Measured as the largest centre to centre distance in the sagittal plane (Figs 2*g*, 3*b*, 5 *l*).

COw. Width of the basal turn of the cochlea. Measured as the largest centre to centre distance in the transverse plane (Figs 1*h*, 3*a*, 5*f*).

Note: no accurate and reproducible measurements of the length, breadth, or height of the vestibule could be defined.

Orientations – labyrinth

ASCs. Orientation of the most superior part of the anterior semicircular canal in the transverse plane. Measured in its midline (Figs 1*a*, 3*c*, 5*a*).

ASCm. Orientation in the transverse plane of the arc of the anterior semicircular canal at its largest width. Defined by the line connecting the landmarks of ASCw (Figs 1*c*, 3*c*, 4*d–f*, 5*b*). This measurement approximately represents the average orientation of the anterior semicircular canal in the transverse plane.

V. Orientation of the vestibule in the transverse plane. Defined by the line connecting the centres of the apertures of the ampulla of the anterior semicircular canal and the common crus into the vestibule (Figs 1*e*, 3*c*, 5*c*). This line was found to give the best reproducible orientation of the vestibule. This measurement also represents the orientation of the most inferior part of the arc of the anterior semicircular canal, and therefore the difference between ASCs and V quantifies the degree of torsion of the anterior semicircular canal in the transverse plane.

PSCs. Orientation in the superior limb of the posterior semicircular canal in the transverse plane. Measured in its midline (Figs 1*c*, 3*c*, 5*b*).

PSCm. Orientation in the transverse plane of the arc of the posterior semicircular canal at its greatest height. Defined by the line connecting the landmarks of PSCh (Figs 1*e*, 3*c*, 5*c*). This measurement represents the average orientation of the posterior semicircular canal in the transverse plane.

PSCi. Orientation of the inferior limb of the posterior semicircular canal in the transverse plane. Measured in its midline (Figs 1*h*, 3*c*, 5*f*). The difference between PSCs and PSCi quantifies the degree of torsion of the posterior semicircular canal in the transverse plane.

LSCt. Orientation of the lateral semicircular canal in the transverse plane. Defined by the line connecting the landmarks of LSCh (Figs 1*f*, 3*c*, 4*a*, 5*d*).

LSCl. Orientation of the most lateral part of the lateral semicircular canal in the sagittal plane. Measured in its midline (Figs 2*a*, 3*d*, 5*g*).

LSCm. Orientation of the lateral semicircular canal in the sagittal plane. Measured at the largest sagittal centre to centre diameter of its arc. The anterior landmark is usually located in the ampulla of the canal (Figs 2*c*, 3*d*, 5*h*). The plane parallel to this orientation and perpendicular to the (mid) sagittal plane approximately corresponds to the transverse plane used in this study. The orientation of the lateral semicircular canal in the sagittal plane has been used as reference plane in craniological studies by Perez (1922), Girard (1923, 1947), Lebedkin (1924), Saban (1952), Sercer & Krmpotic (1958), Delattre & Fenart (1960) and others listed in Fenart & Pellerin (1988). The difference between LSCl and LSCm quantifies the degree of torsion of the lateral semicircular canal in the sagittal plane.

CCR. Orientation of the common crus in the sagittal plane. Measured in its midline. This measurement is illustrated and briefly mentioned by Werner (1933, 1960), Delattre & Fenart (1962) and Fenart & Deblock (1973) (Figs 2*e*, 3*d*, 5*j*).

APA. Orientation of the ampullar line connecting the centres of the ampullae of the anterior semicircular canal and posterior semicircular canal projected on the sagittal plane (Figs 2*c*, *e*, 3*d*, 5*h*, *j*). As both landmarks never occur in a single sagittal scan the orientation must be calculated using the x, y co-ordinates of the 2 ampullar landmarks. This ampullar line was illustrated and described by Werner (1933, 1960). However, Delattre (1951) and Fenart & Deblock (1973: 63) incorrectly state that the orientation of this line is similar to the intersection of the midsagittal plane and the plane through the 3 ampullae used by Villemin & Beauvieux (1934) and Robin et al. (1968).

COs. Orientation of the basal turn of cochlea in the sagittal plane. Defined by the line connecting the landmarks of COh (Figs 2*g*, 3*d*, 5*l*).

COt. Orientation of the basal turn of the cochlea in the transverse plane. Defined by the line connecting the landmarks of COw (Fig. 1*h*, 3*c*, 5*f*).

VC. Orientation of the vestibulocochlear line. Defined by the line connecting the most lateral point of the second turn of the cochlea (pixel with the extreme CT number) and the internal vestibion, projected on the sagittal plane (Fig. 3*d*). The internal vestibion ('vestibion interne') is defined as the centre of the arc of the lateral semicircular canal (Perez, 1922), and in the sagittal scans it is equidistant between the landmarks of the orientation of the lateral semicircular canal (LSCm). Hence, the orientation of the line is calculated from the x, y coordinates of these landmarks (Figs 2*c*, 5*h*) and those of the cochlear point (Figs 2*f*, 5*k*). This measurement, illustrated and briefly discussed by Delattre & Fenart (1961), describes the position of the cochlea relative to the vestibule and the level of the lateral semicircular canal, but not the orientation of the modiolus as defined by Delattre (1951).

Orientations—petrous pyramid

CC. Orientation of the petrous part of the carotid canal in the transverse plane. Measured in its estimated midline (Figs 1*j*, 5*m*). In the present study measured from $\times 2$ magnified scans.

FC2. Orientation of the second part (tympanic portion) of the facial canal in the transverse plane. Measured from its anterior hiatus to the transition into its third part (mastoid portion) (Figs 1*h*, 5*n*).

FC3. Orientation of the third part of the facial canal in the sagittal plane. Measured from the centre of the stylomastoid foramen to the transition into its second part (Figs 2*a*, 5*o*).

PPsp. Orientation of the superior part of the posterior petrosal surface in the transverse plane. Measured at level of the most superior part of the anterior semicircular canal (ASCs) and defined as the line from the anterior margin of the sigmoid sulcus to the most anteriomedial point of the posterior surface visualised in the scan (Figs 1*a*, 5*p*). In the present study measured from unmagnified scans.

PPip. Orientation of the inferior part of the posterior petrosal surface in the transverse plane. Measured at the level of the lateral semicircular canal (see LSCh,w,t) and defined as the tangent touching both the anterior margin of the internal acoustic meatus and the anterior margin of the sigmoid sulcus (Fig. 1*f*, 5*q*). The use of these landmarks reduces the influence of the irregular posterior petrosal surface, caused by retrolabyrinthine pneumatisation, on the measurement. In the present study measured from unmagnified scans.

PPa. Orientation of the anterior petrosal surface in the sagittal plane. Measured at the level of the common crus (see CCR) and defined as the line connecting the anterior margin of the superior petrosal sinus and the petrosquamous or sphenopetrosal suture (Figs 2*e*, 5*r*).

PPp. Orientation of the posterior petrosal surface in the sagittal plane. Measured at the level of the common crus and defined as the line connecting the posterior margin of the superior petrosal sulcus and the superior margin of the sigmoid sulcus (Figs 2*e*, 5*r*). The use of these landmarks reduces the influence of the irregular posterior petrosal surface, caused by retrolabyrinthine pneumatisation, on the measurement.

Note: No consistent method of measuring the orientation of the anterior petrosal surface in the transverse plane could be defined.

Indices

TLI. Transverse labyrinthine index. calculated from the transverse scan which best displays the complete extent of the lateral semicircular canal (see LSCh,w,t). It describes the relative division of the line between the centre of the ampulla of the lateral semicircular canal and the centre of the posterior semicircular canal in this scan by the centre of the posterior limb of the lateral semicircular canal. It is defined as the length of the posterior part of this line given as a percentage of the total line length (Figs 1*f*, 3*c*, 5*e*; $\text{TLIp}/\text{TLIa}+\text{TLIp} \times 100$). This index expresses a combination of the relative size and orientation of the arcs of the lateral and posterior semicircular canals in the transverse plane, which appears to distinguish the human labyrinth from that of other primates.

SLI. Sagittal labyrinthine index. This index is based on the observation by Hyrtl (1845) and Gray (1907) that, if seen in lateral view, the plane of the lateral semicircular canal divides the arc of the posterior semicircular canal into about equal halves in anthropoids, whereas the lateral semicircular canal is more inferiorly positioned in some new world monkeys and prosimians. The SLI is defined as the percentage of the width of the posterior semicircular canal (PSCw) that is situated below the plane through the orientation of the lateral semicircular canal (LSCm) perpendicular to the sagittal plane (Figs 2*c*, *d*, 3*d*, 5*i*; $\text{SLIi}/\text{SLIs}+\text{SLI} \times 100$). It is calculated from the coordinates of the landmarks of PSCw and LSCm.